Growth Model for Bamboolike Structured Carbon Nanotubes Synthesized Using Thermal Chemical Vapor Deposition

Cheol Jin Lee*

School of Electrical Engineering, Kunsan National University, Kunsan 573-701, S. Korea

Jeunghee Park

Department of Chemistry, Korea University, Jochiwon 339-700, S. Korea

Received: September 13, 2000; In Final Form: January 8, 2001

Carbon nanotubes (CNTs) are grown vertically aligned on Fe catalytic particles deposited on a silicon oxide substrate at temperatures ranging from 550 to 950 °C by thermal chemical vapor deposition of acetylene. All CNTs have a bamboolike structure in which the curvature of compartment layers is directed toward the tip, irrespective to the growth temperature. Most of tips are closed and free from the encapsulation of Fe particle. However, the CNTs grown at 550 °C sometimes encapsulate the Fe particle at the closed tip. On the basis of experimental results, we provide a detailed growth model for the bamboolike structured CNTs grown using thermal chemical vapor deposition.

Introduction

Since discovered by Iijima,[1] research on the carbon nanotubes (CNTs) has attracted a lot of attention in the past decade due to their important applications. For example, the CNTs can be used as electron field emitters of flat panel displays,[2,3] atomic force microscope/scanning tunneling microscope probes,[4] and hydrogen storagers.[5] However, many possible applications require mass production of high-quality CNTs. To date, various synthetic methods, e.g. arc discharge,[6,7] laser vaporization,[8] pyrolysis,[9] and plasma-enhanced[10] and thermal chemical vapor deposition (CVD),[11,12] have been developed. Recently, the synthesis of CNTs using the CVD method has been extensively studied because of relatively lower growth temperature (below 1000 °C) compared to arc-discharge or laser vaporization methods. Moreover, the CVD method offers a route to control over the diameter, length, and alignment of CNTs.

Understanding of the growth mechanism of CNTs would help in controlled growth and development of new synthesis methods. However, the complexity of the growth process makes it difficult to investigate at the molecular level. Given the different synthetic techniques, a variety of growth mechanisms were suggested. In the syntheses using plasma-enhanced CVD, the catalytic particles were usually encapsulated at the tip of CNTs,[10,13,14] which was explained by adopting a tip growth mechanism.[15] Wang and co-workers reported the capped Fe catalytic particles in the bambooshaped CNTs synthesized by the pyrolysis method and proposed a tip growth mechanism involving two sized catalytic particles.[16] In contrast, Dai and co-workers suggested a base growth mechanism that the CNTs grow upward from the metal particles attached to the substrate.[12,17]

In the present work, we have grown the vertically aligned CNTs on Fe-deposited SiO_2 substrate in a wide temperature range 550−950 °C by thermal CVD of acetylene (C_2H_2). Transmission electron microscope images reveal that all CNTs have a bamboolike structure independently of growth temperature. The curvature of compartment layers in the bamboolike structure is always directed to the tip. It is also found that the tips are closed and usually not encapsulated with catalytic particles except a small fraction of CNTs grown at 550 °C, which is different from those grown by plasma-enhanced CVD and pyrolysis methods. Therefore, we propose a base growth model for the bamboo-shaped CNT growth using thermal CVD.

Experimental Section

The 20 mm × 30 mm size p-type Si(100) substrates with a resistivity of 15 Ω·cm were thermally oxidized. The thickness of silicon oxide (SiO_2) layer was estimated to be approximately 300 nm. A 100-nm-thick Fe film was thermally deposited on a SiO_2 layer under a pressure of 10^{-6} Torr. The Fe-deposited SiO_2 substrates were dipped in a diluted HF solution for 200 s and then loaded with face down direction on a quartz boat placed in quartz CVD reactor. The deposited Fe film was pretreated at 750−950 °C by NH_3 gas with a flow rate of 100−200 sccm for 20−40 min in order to form the Fe particles in nanometer size. This step is crucial in controlling the size and the vertical alignment of CNTs.[18] The CNTs were grown on the Fe particles using C_2H_2 gas with a flow rate of 40−80 sccm for 10 min at 600, 750, 850, and 950 °C.

As the growth temperature decreases to below 600 °C, the growth of CNTs was not successful by using the procedure described above. Therefore, for the growth at 550 °C we used a modified CVD reactor that consists of two different temperature zones heated separately by resistive heating coils.[19] The first and second heating zones were maintained at 850 and 550 °C, respectively. The Fe/SiO_2 substrates were loaded on a quartz boat placed in the second heating zone. The reactants heated in the first heating zone are brought into the second heating zone for the CNT growth.

The CNTs were examined by a scanning electron microscope (SEM) (Hitachi S600) to measure the alignment, configuration, and diameter distribution of CNTs. A transmission electron

* To whom correspondence should be addressed. E-mail: cjlee@ks.kunsan.ac.kr.

10.1021/jp0032762 CCC: $20.00
Published on Web 03/03/2001

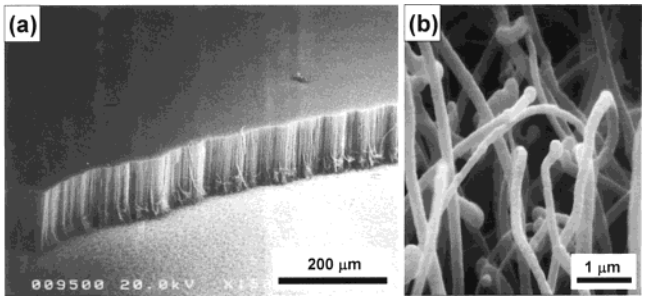

Figure 1. SEM micrographs of vertically well-aligned CNTs grown on Fe-deposited SiO_2 substrate at 950 °C: (a) uniformly grown CNT with a length of 100 μm; (b) magnified top view showing the diameters in the range 100−200 nm and the closed tips.

microscope (TEM) (Philips CM20T, 200 kV) was used to investigate the structure of CNTs. TEM analysis was performed on the CNTs dispersed on a carbon TEM microgrid after separating from the substrate by ultrasonic treatment in acetone.

Results

Figure 1 shows SEM micrographs for the vertically well-aligned CNTs grown on Fe-deposited SiO_2 substrate, under the condition that C_2H_2 gas flows with a rate of 40 sccm for 10 min at 950 °C. The CNTs are grown with an uniform length of 100 μm. A magnified top view, as shown in Figure 1b, reveals the diameters in the range 100−200 nm, closed tips, and clean surface without any carbonaceous particles. The tips are tilted with a few degree angles from vertical direction. The CNTs grown at 850, 750, 600, and 550 °C are vertically aligned on the substrate as well, while the length and diameter are dependent on the growth temperature.[19,20]

Figure 2a−e shows TEM images of the CNTs grown at 950, 850, 750, 600, and 550 °C, respectively. The CNTs have a bamboolike structure over the wide temperature range. The TEM images reveal the closed tip without any encapsulated Fe particles (see arrows ①) and the compartment layers whose curvature is directed toward the tip (see arrows ②). Open roots separated from the Fe particles are found (see arrows ③). The inset of Figure 2c clearly shows that the CNT grown at 750 °C has no encapsulated Fe particle at the closed tip and the compartment layers with a curvature directed to the tip. In Figure 2e, the majority of tips are free of encapsulated Fe particle, but some of the tips are encapsulated with Fe particles (see arrows ④), which were not found from the CNTs grown at higher temperatures. The diameters of CNTs grown at 600−950 °C are widely distributed in the range from 50 to 300 nm, but those of CNTs grown at 550 °C are uniformly distributed in the range 20−30 nm. The average of diameters decreases with decreasing growth temperature.

Figure 3a is a high-resolution TEM (HRTEM) image showing the bamboolike structure of CNT grown at 950 °C. The crystalline graphitic sheets of wall (indicated by arrow ①) combine with those of compartment layer (indicated by arrow ②), resulting in an increase of wall thickness. There are some defective graphitic sheets at the surface of wall as indicated by arrow ③. Figure 3b is a TEM image of the bamboo-shaped CNTs grown at 550 °C, clearly showing an Fe-particle-free tip (see arrow ①) and an Fe-particle encapsulated tip (see arrow ②). The curvature of compartment layers is oriented to the closed tip, regardless of Fe-particle encapsulation (see arrows ③). The crystallinity of graphitic sheets is much worse than that of CNTs grown at 950 °C.

Figure 4 is a HRTEM image for the wall of a CNT grown at 950 °C. There is a joint between the wall (indicated by arrow

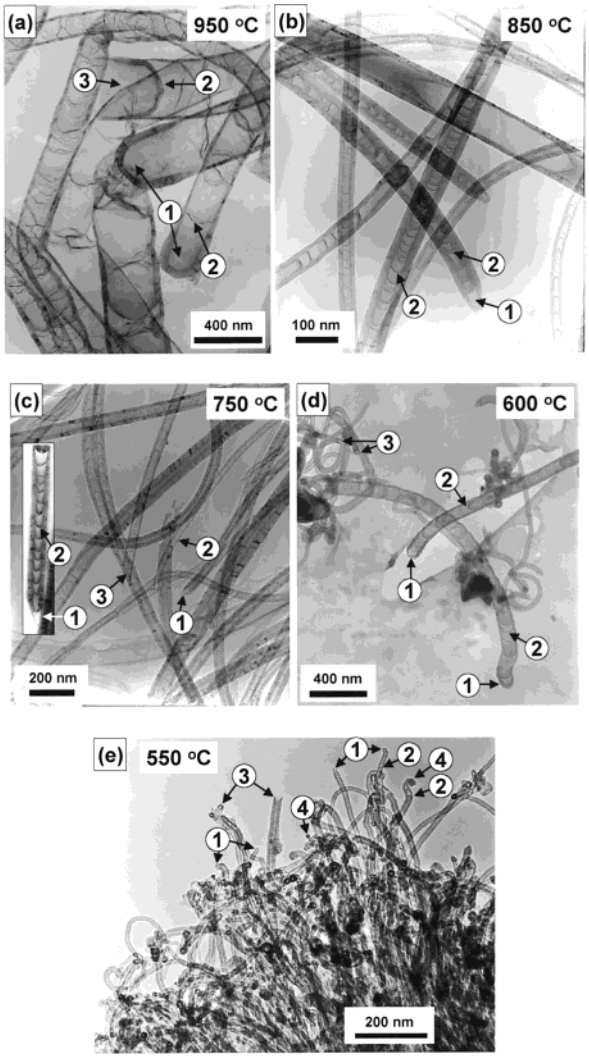

Figure 2. TEM images of CNTs grown at (a) 950 °C, (b) 850 °C, (c) 750 °C, (d) 600 °C, and (e) 550 °C. All CNTs exhibit a bamboolike structure. The arrows ① indicate the closed tips with no encapsulated Fe particle. The arrows ② correspond to the compartment layers whose curvature is directed to the tip. The arrows ③ indicate the open roots separated from Fe particles. The arrows ④ in (e) indicate the Fe-particle encapsulated tips.

①) and the compartment layer (indicated by arrow ②). The number of graphitic sheets at the wall is significantly influenced by the presence of joint. If one follows the downward direction (see the marked positions), the wall thickness reduces from 9 to 6 nm and increases to 9 nm after a joint with compartment layer, subsequently decreasing to 8 nm. The crystalline graphitic sheets of wall combine with those of compartment without any defects as indicated by arrow ③. Despite the change in wall thickness, the outer diameter remains almost same. The graphitic sheets of wall are aligned to the tube axis with an angle of about 5° (see △ and ◇ marks). The crystalline graphitic sheet (indicated by mark △) becomes defective and finally vanishes at the outside as indicated by arrow ④. The outer graphitic sheets continuously disappear along the tube.

Discussion

The present experimental results show that all CNTs grown at temperatures ranging from 550 to 950 °C have the bamboolike structure in which the curvature of compartment layer is directed toward the closed tip. The bamboo-shaped CNTs were synthesized using arc discharge,[21−25] pyrolyis,[16] vapor phase growth,[26]

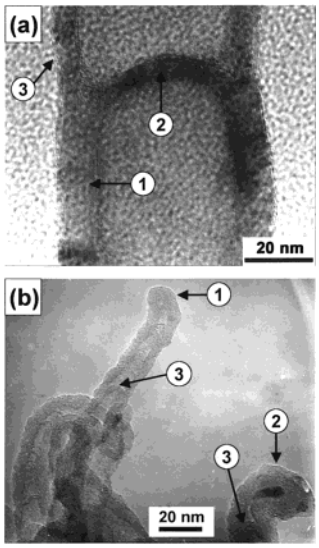

Figure 3. (a) HRTEM image for the bamboolike structure of CNT grown at 950 °C. The wall (indicated by arrow ①) connects with the compartment layers (indicated by arrow ②), resulting in increasing the wall thickness. The arrow ③ indicates defective graphitic sheets at the surface of wall. (b) TEM image of bamboo-shaped CNTs grown at 550 °C, showing an Fe-particle free tip (see arrow ①) and an Fe-particle encapsulated tip (see arrow ②). The curvature of compartment layers has a direction toward the tip for both CNTs (see arrows ③).

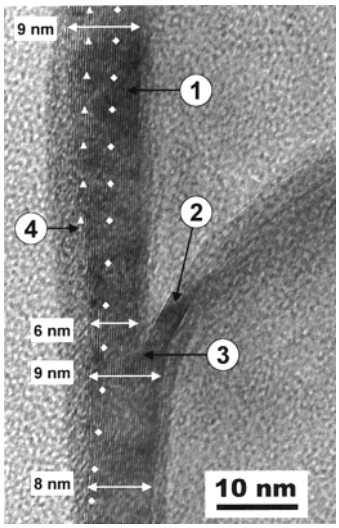

Figure 4. HRTEM image for the wall of a CNT grown at 950 °C, showing a joint between the wall (indicated by arrow ①) and the compartment layer (indicated by arrow ②). Following the downward direction, the thickness of wall changes (see arrow-marked positions). The graphitic sheets of wall combine with those of compartment without any defects as indicated by arrow ③ and are aligned to the tube axis with a tilted angle of about 5° (see △ and ◇ marks). The crystalline graphitic sheet (indicated by mark △) becomes defective and finally vanishes at the outside as indicated by arrow ④.

and plasma-enhanced CVD.[13] However, the curvature of compartment layer in the bamboo-shaped CNTs grown using plasma-enhanced CVD and pyrolysis methods is directed to the root, which is opposite to that of our present works. As mentioned in the Introduction, the tips of those CNTs are encapsulated with catalytic particle, which was justified by tip growth mechanism. On the other hand, base growth mechanism would be adequate to describe the closed tips that are free of encapsulated catalytic particles as well as the compartment curvature directed to the tip. The base growth model is apparently inconsistent with the catalytic-particle encapsulated tips of CNTs grown at 550 °C. However, since the curvature of compartment layers is directed to the tip for all CNTs, irrespective to the encapsulation of catalytic metal, the base growth model can be applicable. We suggest that the encapsulated Fe particle may not participate in overall growth process. Encapsulation of catalytic metal particles has been explained by the occurrence of melting at the metal surface due to the size effect and the interfacial effect between metal and graphite.[17,24,26,27] We noted that the outer diameter of CNTs grown at 600, 750, 850, and 950 °C is at least larger than 50 nm, while it is narrower than 30 nm for the CNTs grown at 550 °C. A greater decrease of melting point is expected for smaller Fe particles, and thus, the melted Fe particles are possibly encapsulated in narrower CNTs.

Saito and Yoshikawa reported a TEM image of bamboo-shaped CNTs grown by arc discharge.[21] One end of the tube is capped with Ni catalytic particle, and the curvature of conical compartment layers is oriented to the opposite of the Ni particle. A growth model was suggested that the dissolved carbons diffuse into the bottom of the conical Ni particles, segregating as graphite at the bottom and the side of the Ni particles.[28] Our HRTEM images are incorporated with their results, in which the graphitic sheets of wall are tilted with an angle of few degrees to the tube axis and the graphitic sheets at the outside continuously extinct. There is more work to conjecture the growth model of bamboo-shaped CNTs particularly grown by arc discharge.[23−25,29]

The base growth model was early developed for catalytic carbon filament growth by Baker et al.[30] They concluded that the filament can grow upward from the metal particles that remain attached to the substrate. The Dai group suggested that the growth of vertically aligned multiwalled CNTs using thermal CVD of ethylene at 700 °C follows the base growth mechanism.[12] They also suggested a base growth of single-walled CNTs grown using CVD of methane, based on the TEM image of closed tube ends that are free of attached or encapsulated metal particles.[17]

Here we present a base growth model of bamboo-shaped CNTs, which comprises the following structural features observed from TEM images. There is no encapsulated catalytic metal particle at the closed tip. The curvature of the compartment layer in the bamboolike structure is directed to the tip. The graphitic sheets at the wall are aligned to the tube axis with an angle of few degrees. The compartment joins with the wall without any defects, resulting in increasing the wall thickness. The outer graphitic sheets continuously vanish along the tube, so the outer diameter remains almost same.

Schematic diagrams of the base growth model are shown in Figure 5. Carbons produced from the decomposition of C_2H_2 adsorb on the catalytic metal particle. Then they diffuse via surface and bulk of metal particle to form the graphitic sheets as a cap on the catalytic particle (see Figure 5a). The formation of hexagons may be catalytically promoted by the assistance of the catalytic metal particle.[31] As the cap lifts off the catalytic particle, a closed tip with inside hollow is produced (see Figure 5b). The motive force departing from the catalytic particle may be the stress accumulated under the graphitic cap. The size of catalytic particle limits the diameter of growing tube. Since the wall grows toward the vertical direction with a few degrees angles, the outer graphitic sheets disappear continuously due to the pushing-out force from the reaction site of catalytic particle. The carbons accumulated at the inside surface of catalytic particle, probably mainly via bulk diffusion, can form the compartment graphitic sheets. The compartment graphitic

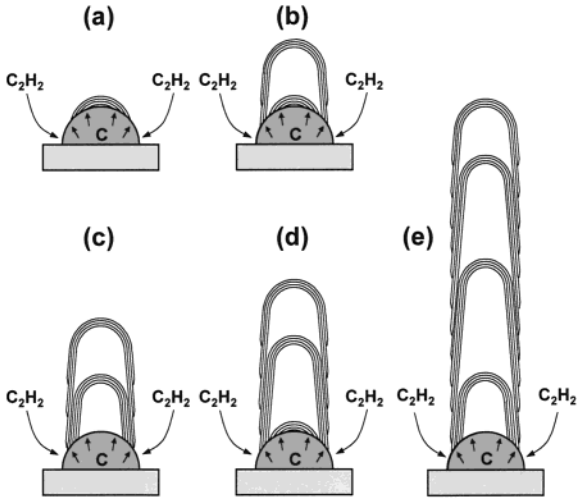

Figure 5. Schematic diagrams of a base growth model.

sheets would grow by joining with the graphitic sheets of wall, resulting in an increase of wall thickness at the joint part. The compartment layer will depart from the catalytic particle due to the stress (see Figure 5c). While the wall grows upward, the next compartment layer is produced on the catalytic particle and will be combined with the wall (see Figure 5d). If the carbons are supplied under steady-state conditions, the compartment layers can appear periodically (see Figure 5e). However, nonuniform carbon supply would result in an irregular appearance of compartment layers with various thicknesses and shapes.

Conclusion

We have reported the structural features of vertically aligned CNTs grown on an Fe-deposited SiO_2 substrate at temperatures ranging from 550 to 950 °C by thermal CVD of C_2H_2. All of the CNTs have a bamboolike structure in which the curvature of compartment layers is directed to the tip, independently of the growth temperature. The CNTs grown at 950, 850, 750, and 600 °C have a diameter in the range 50−300 nm and no encapsulated Fe particles at the closed tip. The CNTs grown at 550 °C have a diameter of 20−30 nm and sometimes encapsulate Fe particles at the closed tip, which can be explained by a melting of Fe particles due to the nanometer size. However, since the curvature of compartment layers is directed to the tip for all CNTs irrespective to the encapsulation of catalytic particles, the same base growth model can be applicable. The HRTEM images reveal that the graphitic sheets of wall combine with those of the compartment to increase the wall thickness. They are aligned to the tube axis with an angle of few degrees and disappear at the outside. On the basis of these experimental results, we propose a base growth model for the bamboolike structured CNTs. The growth model illustrates whereby the wall grows toward vertical direction and connects periodically with the compartment layers. Our growth model would provide an insight into understanding the complicated growth process of CNTs.

References and Notes

(1) Iijima, S. *Nature* **1991**, *354*, 56.
(2) de Heer, W. A.; Chatelain, A.; Ugarte, D. *Science* **1995**, *270*, 1179.
(3) Saito, Y.; Hamaguchi, K.; Hata, K.; Uchida, K.; Tasaka, Y.; Ikazaki, F.; Yumura, M.; Kasuya, A.; Nishina, Y. *Nature* **1997**, *389*, 554.
(4) Dai, H.; Hafner, J. H.; Rinzler, A. G.; Colbert, D. T.; Smalley, R. E. *Nature* **1996**, *384*, 147.
(5) Liu, C.; Fan, Y. Y.; Liu, M.; Cong, H. T.; Cheng, H. M.; Dresselhaus, M. S. *Science* **1999**, *286*, 1127.
(6) Bethune, D. S.; Kiang, C. H.; deVries, M. S.; Gorman, G.; Savoy, R.; Vazquez, J.; Beyers, R. *Nature* **1993**, *363*, 605.
(7) Journet, C.; Maser, W. K.; Bernier, P.; Loiseau, A.; Lamy de la Chapelle, M.; Lefrant, S.; Deniard, P.; Lee, R.; Fischer, J. E. *Nature* **1997**, *388*, 756.
(8) Thess, A.; Lee, R.; Nikolaev, P.; Dai, H.; Petit, P.; Robert, J.; Xu, C.; Lee, Y. H.; Kim, S. G.; Rinzler, A. G.; Colbert, D. T.; Scuseria, G. E.; Tomanek, D.; Fisher, J. E.; Smalley, R. E. *Science* **1996**, *273*, 483.
(9) Terrones, M.; Grobert, N.; Olivares, J.; Zhang, J. P.; Terrones, H.; Kordatos, K.; Hsu, W. K.; Hare, J. P.; Townsend, P. D.; Prassides, K.; Cheetham, A. K.; Kroto, H. W.; Walton, D. R. M. *Nature* **1997**, *388*, 52.
(10) Ren, Z. F.; Huang, Z. P.; Xu, J. W.; Wang, J. H.; Bush, P.; Siegal, M. P.; Provencio, P. N. *Science* **1998**, *282*, 1105.
(11) Li, W. Z.; Xie, S. S.; Qian, L. X.; Chang, B. H.; Zou, B. S.; Zhou, W. Y.; Zhao, R. A.; Wang, G. *Science* **1996**, *274*, 1701.
(12) Fan, S.; Chapline, M. G.; Franklin, N. R.; Tombler, T. W.; Cassell, A. M.; Dai, H. *Science* **1999**, *283*, 512.
(13) Murakami, H.; Hirakawa, M.; Tanaka, C.; Yamakawa, H. *Appl. Phys. Lett.* **2000**, *76*, 1776.
(14) Chen, Y.; Shaw, D. T.; Guo, L. *Appl. Phys. Lett.* **2000**, *76*, 2469.
(15) Baker, R. T. K. *Carbon* **1989**, *27*, 315.
(16) Li, D.-C.; Dai, L.; Huang, S.; Mau, A. W. H.; Wang, Z. L. *Chem. Phys. Lett.* **2000**, *316*, 349.
(17) Cassell, A. M.; Raymakers, J. A.; Kong, J.; Dai, H. *J. Phys. Chem.* **1999**, *103*, 6484.
(18) Lee, C. J.; Kim, D. W.; Lee, T. J.; Choi, Y. C.; Park, Y. S.; Kim, W. S.; Lee, Y. H.; Choi, W. B.; Lee, N. S.; Kim, J. M.; Choi, Y. G.; Yu, S. C. *Appl. Phys. Lett.* **1999**, *75*, 1721.
(19) Lee, C. J.; Son, K. H.; Park, J.; Yoo, J. E.; Huh, Y.; Lee, J. Y. *Chem. Phys. Lett.*, submitted for publication.
(20) Lee, C. J.; Park, J. H.; Park, J. *Chem. Phys. Lett.* **2000**, *323*, 560.
(21) Saito, Y.; Yoshikawa, T. *J. Cryst. Growth* **1993**, *134*, 154.
(22) Okuyama, F.; Ogasawara, I. *Appl. Phys. Lett.* **1997**, *71*, 623.
(23) Kovaleski, V. V.; Safronov, A. N. *Carbon* **1998**, *36*, 963.
(24) Kukovitsky, E. F.; L'vov, S. G.; Sainov, N. A. *Chem. Phys. Lett.* **2000**, *317*, 65.
(25) Blank, V. D.; Gorlova, I. G.; Hutchison, J. L.; Kiselev, N. A.; Ormont, A. B.; Polyakov, E. V.; Sloan, J.; Zakharov, D. N.; Zybtsev, S. G. *Carbon* **2000**, *38*, 217.
(26) Li, Y.; Chen, J.; Ma, Y.; Zhao, J.; Qin, Y.; Chang, L. *Chem. Commun.* **1999**, 1141.
(27) Wang, Z. L.; Petroski, J. M.; Green, T. C.; El-Sayed, M. A. *J. Phys. Chem. B* **1998**, *102*, 6145.
(28) Saito, Y. *Carbon* **1995**, *33*, 979.
(29) Louchev, O. A.; Sato, Y. *Appl. Phys. Lett.* **1999**, *74*, 194.
(30) Baker, R. T. K.; Chludzinski, J. J. *J. Phys. Chem.* **1986**, *90*, 4.
(31) Lee, Y. H.; Kim, S. G.; Tománek, D. *Phys. Rev. Lett.* **1997**, *78*, 734, 2393.